Viewing Quality Enhancement of 3D Reconstructed Images in Computational Integral Imaging Reconstruction by use of Averaging Method

Gen Li, Dong-Choon Hwang,Keong-Jin Lee and Eun-Soo Kim
3D Display Research Center, Dept. of Electronic Engineering, Kwagnwoon Univ., 447-1 Wolge-Dong, Nowon-Gu, Seoul, Seoul 139-701, Korea
TEL:82-2-940-5520, e-mail: theligen@gmail.com.
Keywords : 3D Display, integral imaging, elemental image, CIIR

Abstract

In this paper, an improved computational integral imaging reconstruction (CIIR) is proposed. The proposed method can highly enhance the viewing quality of reconstructed image. To show the feasibility of proposed method, some experiments are performed and the results are compared and discussed with those of the conventional method.

1. Introduction

The integral imaging scheme has been regarded as a promising technique for implementation of the next-generation three-dimensional (3-D) imaging and display system because it can provide full-parallax and continuous-viewing 3-D images without a convergence-accommodation conflict.

Basically, the integral imaging system is composed of two processes: pickup and reconstruction [1]. In the pickup process, de-magnified object images with different perspectives of the 3-D object called elemental images are recorded as a form of the elemental image array (EIA). In the reconstruction process, the recorded elemental images are displayed on a display panel and then the 3-D image can be reconstructed and observed through a lenslet array.

Recently, two kinds of reconstruction methods have been studied for 3-D image display. One is optical integral imaging reconstruction (OIIR), and the other is computational integral imaging reconstruction (CIIR). In OIIR method, resolution and image quality of the reconstructed 3-D images appear to be low and degraded due to physical limitations of the employed optical devices such as diffraction, aberration and non-uniformity.

In contrast, in the CIIR method 3-D images as a form of depth-dependent plane object images (POIs) along the output plane are computationally reconstructed via digital simulation of ray optics [2]. This property of CIIR is useful in partially occluded object recognition.

However, because the convention CIIR method is based on simulation model of the optical display process, the reconstructed 3-D images suffer some problems: intensity degradation around its boundary area, brightness degradation as the reconstructed output distance is getting longer, and intensity irregularity in its center area, etc. The reason for these problems is that the number of overlapped pixels in the reconstructed image plane is insufficient and overlapped pixels are unevenly distributed.

In this paper, an improved CIIR method is proposed to enhance the viewing-quality of the reconstructed object images. To show the usefulness of proposed method, some experiments are carried out and their results are presented.

2. Overview of conventional CIIR

Figure 1 shows an operational principle of the conventional CIIR technique based on a virtual pinhole model [2]. Firstly, each elemental image in the EIA is inversely mapped through its corresponding pinhole. Secondly, in case an POI is reconstructed on the output plane of z from the pinhole array, each inversely mapped elemental image is digitally magnified by the factor of $M=z/g$, in which z is the distance from the reconstructed image plane to the virtual pinhole array and g is from EIA to the virtual pinhole array. In this mapping process, the distance from pixel position to its mapping position in the reconstructed plane is employed to simulate the intensity attenuation in OIIR. In other words, each mapped pixel on POI is divided by M^2, because light intensity is inverse proportional to its illuminating area. Thirdly, all of the magnified elemental images are overlapped and summed at the corresponding pixels of the reconstructed image plane. Then, a POI

of the 3-D object at the output distance of z can be finally reconstructed. Repeat the process above by varying the output distance value of z, a set of POIs can be reconstructed along the z axis.

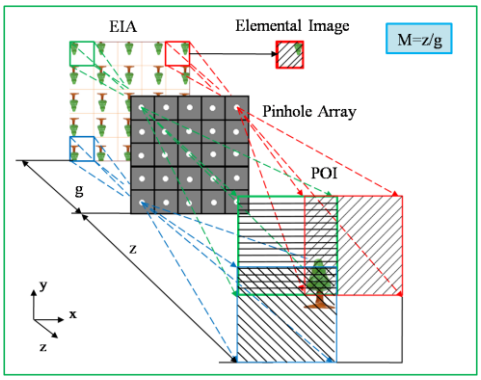

Fig. 1. CIIR based on pinhole array model.

Fundamentally, there is uneven overlapping of elemental images in the reconstructed POIs due to the overlap. Therefore, simulation of the light attenuation might cause poor visual quality of POIs reconstructed by conventional CIIR method.

For analysis of this overlapping process, here we introduce an overlap expectation function of $floor(M)^2$, in which M is a magnification factor used in the CIIR mentioned above. The $floor(X)$ represents a function to obtain the greatest integer less than or equal to X.

The POI can be divided into two kinds of areas: sufficient overlapped area (SOA) and insufficient overlapped area (ISOA). That is, the area, where the number of overlapped pixels in the reconstructed POI is not less than the overlap expectation $floor(M)^2$ is defined here as the SOA. If not, the area is defined as the ISOA.

Now, consider POIs reconstructed by conventional CIIR method when an EIA of $N \times N$ elemental images and a magnification factor of M are given. There can be three kinds of distributions in numbers of overlapped pixels on the reconstructed POIs as shown in Fig. 2, in which each pixel value (PV) represents the number of overlapped pixels of the projected elemental images in that position.

Fig. 2(a) shows a typical distribution of the number of overlapped pixels in the reconstructed POI under the condition that M is greater than N. In this case, all the overlapped pixel values in the POI must be less than the overlap expectation $floor(M)^2$, so that there can be only the ISOA in the whole POI, and as a result the POI reconstructed by conventional CIIR should have a much lower image intensity than that of the real object image.

Furthermore, Fig. 2(b) and (c) show a distribution of the number of overlapped pixels in the POI under the condition that M is less than N. In this case, there can be the SOA in the center area of the POI and the ISOA in other area surrounding this SOA. However, there are some differences between them. That is, there is only one pixel value of $PV=M^2$ in the SOA of Fig. 2(b) for the case that M is an integer, but in case that M is a fraction there can be three different pixel values in the four adjacent areas of the SOA as shown in Fig. 2(c). This property of distribution might cause the intensity irregularity of reconstructed image by conventional CIIR method.

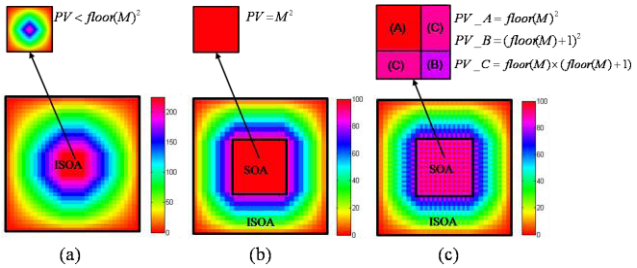

Fig.2.Distributions of the number of the overlapped pixels in the POI under the conditions of (a) M>N, (b) M≤N (M is an integer), (c) M<N (M is a fraction)

3. Proposed scheme

In proposed method, each pixel value of the reconstructed object image is determined as the average of all overlapped pixel values instead of simulating the optical attenuation.

In other words, in the proposed method the number of the overlapped pixels is calculated with a newly employed concept of the pixel-count matrix (PCM). Each pixel of the reconstructed POI is then determined by summing all of the overlapped pixel values and dividing it with the number of the overlapped pixels given by the PCM. In the proposed method each pixel value of the reconstructed POI can be regulated by the calculated PCM, so that the intensity and brightness degradation in the reconstructed POI occurred in the conventional CIIR method can be avoided and as a result its viewing quality will be dramatically improved.

Figure 3 shows a detailed illustration of the proposed method. Let E_{pq} be the elemental image at the p-th row and q-th column in x, y-direction and R be the size of the elemental image. In addition, N_x, N_y, $M=z/g$ are assumed to be the numbers of the

elemental images in the x and y directions and the magnification factor, respectively.

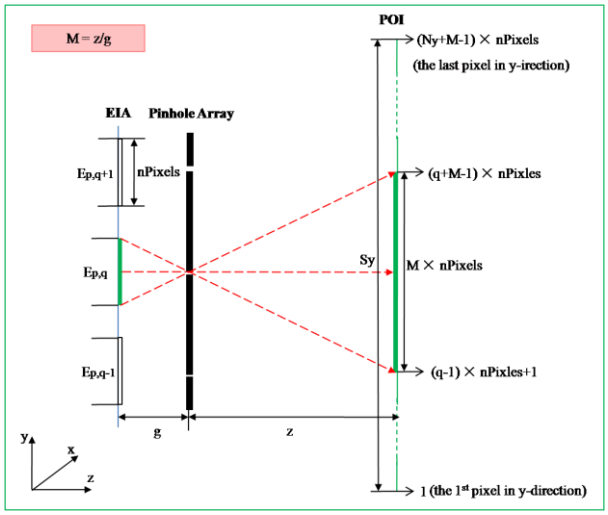

Fig. 3. Mapping diagram of elemental images in the proposed method

Therefore, the size $(S_x,\ S_y)$ of the POI in the x, y-direction can be obtained as described in Eq. (1).

$$\begin{cases} S_x = (N_x + M - 1) \times R \\ S_y = (N_y + M - 1) \times R \end{cases} \tag{1}$$

In the pixel-level overlapping process, there can be only two choices of overlap or no overlap (1 or 0) in each of the vertical and horizontal directions. Therefore, let $PCM_{pq}(x, y, z)$ be the area on the reconstructed output plane of z which is overlapped by the p-th row (x-direction) and q-th (y-direction) column elemental image as shown in Fig. 3. Then, this can be obtained by using Eq. (2).

$$PCM_{pq}(x,y,z) = \begin{cases} 1, if \begin{cases} (p-1)\times R+1 \le x \le (p+M-1)\times R \\ (q-1)\times R+1 \le y \le (q+M-1)\times R \end{cases} \\ 0, else \end{cases} \tag{2}$$

Moreover, let PCM(x, y, z) be the PCM at the distance of z in which each element denotes the number of overlapped pixels, then it can be obtained by using Eq. (3).

$$PCM(x,y,z) = \sum_{p=1}^{N_x} \sum_{q=1}^{N_y} PCM_{pq}(x,y,z) \tag{3}$$

Hence, let Opq(x, y, z) be the inversely magnified elemental image of the p-th row and q-th column on the reconstructed output plane of z. Then, it can be obtained by using Eq. (4).

$$O_{pq}(x,y,z) = E_{pq}\left(R - \frac{x-(p-1)\times R-1}{M\times R}, R - \frac{y-(q-1)\times R-1}{M\times R} \right), \quad \text{for} \begin{cases} (p-1)\times R+1 \le x \le (p+M-1)\times R \\ (q-1)\times R+1 \le y \le (q+M-1)\times R \end{cases} \tag{4}$$

Accordingly, let O(x, y, z) be the reconstructed POI at the distance of z, in which each pixel value of the POI is defined as the average of all overlapped pixel values at that position as shown by Eq. (5).

$$O(x,y,z) = \frac{\sum_{p=1}^{N_x} \sum_{q=1}^{N_y} O_{pq}(x,y,z)}{PCM(x,y,z)} \tag{5}$$

4. Experiments and Results

To evaluate the performance of the proposed CIIR method, some experiments with computationally picked-up elemental images are carried out. Here in the experiment two 2-D objects of 'Tree' and 'House', each located at z_1 and z_2, respectively from the lenslet array are used as a test 3-D object and the gap distance g between the lenslet array and the pickup plane of the elemental images is assumed to be 3 *mm*.

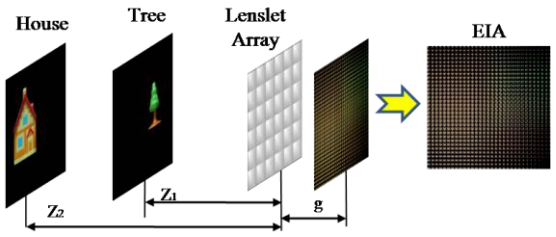

Fig. 4. Experiment setup.

Figure 5 (a) and (b) show the experimental results when z_1=45 *mm* (M=15) and z_2=60 *mm* (M=20). Figure 5 (c) and (d) shows some experimental results when z_1=27 *mm* (M=9) and z_2=42 *mm* (M=14). Figure 6 (e) and (f) shows the experimental results when tree and house are assumed to be located at z_1=16.5 *mm* (M=5.5) and z_2=28.5 *mm* (M=9.5). The EIAs consists of 14x14, 20x20, 20x20 elemental images, respectively in the three experiments. The EIA specifications, which are corresponding to the overlap analysis in Fig. 2, confirm that the POIs only contains ISOA in first experiment (Fig.5 (a) and (b)), and contains both ISOA and SOA in the other

experiments. In Fig. 5, POIs in the first row focus on tree, the POIs in the second row the focus on house.

In Fig.5 (a) and (b), the PSNRs are improved by more than 2dB in the reconstructions of tree and house because in the ISOA, the proposed method can obtain POIs with higher intensity than conventional method. In Fig. 6 (c) and (d), intensity of POIs in the In the SOA (in the white line) are same between the two method. That is because when M is an integer, the POI calculations are same mathematically. However the intensity of POIs in the ISOA (out of the white line) reconstructed by proposed method is higher than that of conventional method because the proposed method can enhance intensity when POIs suffer insufficient overlap. In Fig. 6 (c) and (d), because M is a fraction not an integer, the POIs suffer irregular intensity in the SOA (in the white line). The proposed method can overcome this problem and improve PSNR by more than 7dB and 3dB in the reconstruction of tree and house.

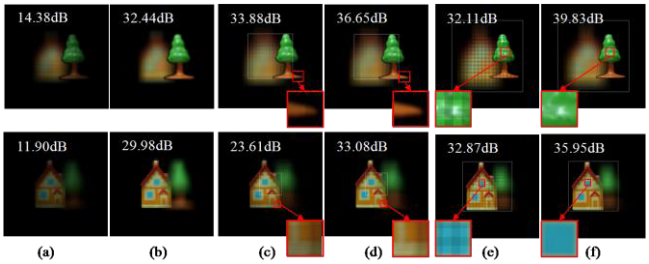

Fig. 5. Reconstructed images by CIIR (a),(c),(d) conventional method, (b),(d),(e), proposed method

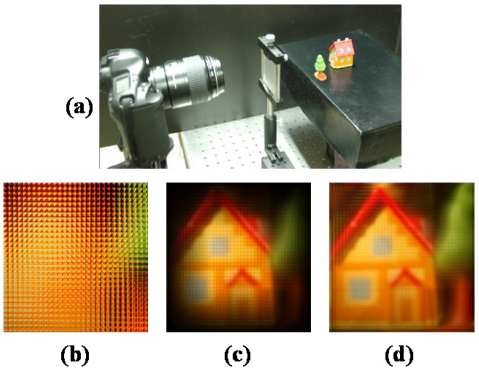

Fig. 6. (a)Optical experiment setup, (b) EIA, (c) reconstructed image by conventional CIIR, (d) reconstructed image by proposed method.

Fig. 6 shows an experiment using optically recorded elemental images of a real object tree and house. They were longitudinally located at z_1=30 *mm* and z_2=50 *mm*, respectively. The lenslet array with 30×30 lenslets was located at z=0 *mm*. The focal length of each lenslet is 3.1 mm and a single elemental image is composed of 66×66 pixels. The experiment setup and optically recorded elemental images are shown in Fig. 6(a) and (b). Figures 6(c) and (d) show the computationally reconstructed images at z=50 mm for the conventional method and the proposed method, respectively. It must be noted here that there is a big difference between the two reconstructed images. In the Fig.6 (c), its boundary area suffers intensity degradation and its center area suffers intensity irregularity by conventional method. The proposed method provides a better result.

5. Summary

The proposed method improved the viewing quality of the reconstructed integral images, which can be used not only in 3-D display fields but also in some applications such as detection and recognition of 3-D objects in a scene [3], and depth and location extraction of 3-D objects in space [4].

Acknowledgements

This research was supported by the MKE (Ministry of Knowledge Economy), Korea, under the ITRC (Information Technology Research Center) support program supervised by the IITA (Institute of Information Technology Assessment) (IITA-2008-C1090-0801-0018).

6. References

[1] A. Stern and B. Javidi, Proceedings of the IEEE 94, 591- 607 (2006).

[2] S.-H. Hong, J.-S. Jang, and B. Javidi, Opt. Express 12, 483-491 (2004).

[3] B. Javidi, R. Ronce-Diaz, and S.-H. Hong, Opt. Lett. 31, 1106-1108 (2006)

[4] D.-C. Hwang, K-J Lee, S-C Kim, E.-S Kim, Opt. Express, vol. 16, pp. 3623-3635, (2008)